



Discovery two potent and new inhibitors of 15-lipoxygenase: (*E*)-3-((3,4-dihydroxybenzylidene) amino)-7-hydroxy-2H-chromen-2-one and (*E*)-O-(4-(((7-hydroxy-2-oxo-2H-chromen-3-yl) imino)methine) phenyl)dimethylcarbamothioate

Carolina Nuñez¹ · Nicole Morales² · Olimpo García-Beltrán^{3,4} · Carolina Mascayano¹ · Angelica Fierro²

Received: 20 February 2017 / Accepted: 19 June 2017 / Published online: 7 July 2017
© Springer Science+Business Media, LLC 2017

Abstract The mechanisms of action and structural determinants of lipoxygenases inhibitors have been explored on several occasions, but many questions remain unanswered, especially about the differences of the inhibition mechanisms and their effect on the selectivity of lipoxygenases isoenzymes. Thus, REDOX mechanism has been proposed in this research to clarify the lipoxygenases inhibition by coumarins derivatives on 15-sLOX. A series of fifteen coumarin derivatives were synthesized and evaluated as 15-lipoxygenase inhibitors. The results showed that some molecules had submicromolar activities and compete with the substrate as we observed by kinetic studies. The most relevant and interesting result was found for compound **6** who showed an inhibitory activity comparable to nordihydroguaiaretic acid a potent and REDOX inhibitor of lipoxygenases (0.17 and 0.29 μM , respectively). Finally, the docking and molecular dynamics studies showed that the

better ligands were accommodated into the binding site being related with those obtained biological data. In addition, our findings contribute at the understanding of inhibitor structural requirements and elucidate the inhibition mechanism of coumarin derivatives on 15-sLOX. Thus, we point to new parameters for the future design of new ligands with potential therapeutic utility where are involved the lipoxygenases enzymes.

Keywords 15-Lipoxygenase · Coumarin derivatives · Kinetic assay · Pseudoperoxidase · SAR study

Introduction

The lipoxygenases (LOX) are enzymes that belong to the non-heme iron-containing dioxygenase family (Ivanov et al. 2010). These enzymes catalyze the stereo- and the regio-specific introduction of molecular oxygen into polyunsaturated fatty acids such as linoleic acid (LA) and arachidonic acid (AA) (Brash et al. 2012). The LOX can be classified according to the position, where the polyunsaturated fatty acid was oxygenated, for example, 5, 8, 12, and 15-LOX (Newcomer and Brash 2015).

The AA is an essential precursor of many eicosanoids or lipid mediators, such as prostaglandins (PG), lipoxins (LX), leukotrienes (LT), hydroxylated polyunsaturated fatty acids (e.g., HETE), thromboxane (TX) and other compounds resulting from AA metabolism. However, deregulation of these enzymes can trigger serious consequences for human health due to their involvement in many diseases (Needleman et al. 1986), as bronchial asthma (Chauhan and Ducharme 2012), atherosclerosis (Wuest et al. 2014),

Electronic supplementary material The online version of this article (doi:10.1007/s00044-017-1968-9) contains supplementary material, which is available to authorized users.

✉ Carolina Mascayano
carolina.mascayano@usach.cl

¹ Facultad de Química y Biología, Departamento de Ciencias del Ambiente, Laboratorio de Simulación Molecular y Diseño Racional de Fármacos, Universidad de Santiago de Chile, Santiago, Chile

² Department of Organic Chemistry, Faculty of Chemistry, Pontificia Universidad Católica de Chile, Casilla 306, Santiago 6094411, Chile

³ Facultad de Ciencias Naturales y Matemáticas, Universidad de Ibagué, Carrera 22 Calle 67, Ibagué 730001, Colombia

⁴ Department of Chemistry, Faculty of Sciences, University of Chile, Santiago 7800024, Chile

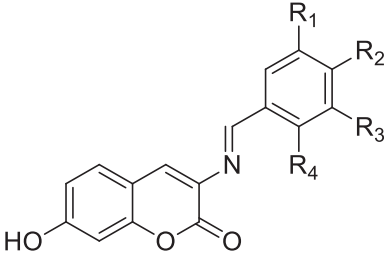
Alzheimer (Giannopoulos et al. 2013), arthritis (Krönke et al. 2009), and certain types of cancer such as: colorectal, prostate and lung (Klil-Drori and Ariel 2013).

Some crystal structures of LOX with good resolution have been elucidated in the last years: i.e., Soybean Lipoxigenase-1 (PDB ID: 1F8N) (Tomchick et al. 2001), soybean lipoxygenase-3 (1HU9) (Skrzypczak-Jankun et al. 2003), rabbit reticulocyte 15-lipoxygenase (1LOX) (Gillmor et al. 1997), coral 8-R-lipoxygenase (2FNQ) (Oldham et al. 2005) and human 5-lipoxygenase (3O8Y) (Gilbert et al. 2011).

All structures show a hydrophobic zone where the fatty acid binds to non-heme iron, which has octahedral coordination geometry; in general, for all LOX's His and Ile residues are found in the active site. Mutations of these residues, for example, in rabbit reticulocyte 15-lipoxygenase (H361, H366, H541, and I663) cause the complete loss of activity, in particular 15-LOX consists of a C-terminal catalytic domain and a N-terminal C2-like β -barrel domain. The catalytic domain contains a non-heme iron in the active site that acts as an electron acceptor or donor during catalysis. During enzyme activation, for example by lipid hydroperoxides, the iron is oxidized from the ferrous state Fe(II) into the ferric Fe(III) form in the active enzyme (Kulkarni et al. 2002).

The search of selective inhibitors of these enzymes is an important target for research (Ribeiro et al. 2014; Armstrong et al. 2014; Sarveswaran et al. 2015). Currently, there is a commercial inhibitor of 5-hLOX called zileuton, which is used in the treatment of asthma (Bell et al. 1992), but there are still not selective inhibitors for 12- and 15-hLOX. For this reason, the study of inhibitors of these isoforms becomes important at present. It has been reported that some important secondary metabolites as flavonoids or isoflavonoids have the ability to inhibit different isoforms of lipoxygenase (Ribeiro et al. 2014). Due to similarities in structure and function, the coumarins are presented as good candidates for LOX inhibitors. There are not many examples of coumarin derivatives as LOX inhibitors (Singh and Pathak 2016; Hoult and Paya 1996; Bansal et al. 2013), but some natural coumarin obtained of *Haplopappus multiflorus* showed to exhibit activity as 15-LOX inhibitors, with over 50% inhibition of the AA lipoperoxidation (Torres et al. 2013) Also, there is evidence that compounds bearing a catechol group such as daphnetin and esculetin block the formation of 5-LOX products with IC₅₀ values between 1.46 and 10 μ M (Yoshiyuki et al. 1985) However, not only catechol coumarins inhibit LOX. The 6-(3-carboxybut-2-enyl)-7-hydroxycoumarin, with only one hydroxyl group, was shown to be a potent inhibitor of 5-LOX (IC₅₀ 36.2 μ M) (Kotali et al. 2016; Hadjipavlou-Litina et al. 2007). Recently, 7-substituted coumarins were synthesized and evaluated in-vitro against 5-LOX obtaining interesting results (Srivastava et al. 2016).

Table 1 Derivatives of (*E*)-3-(benzylideneamino)-7-hydroxy-2*H*-chromen-2-one



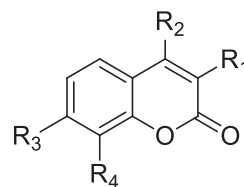
Compounds	R1	R2	R3	R4
1	H	H	H	OH
2	H	OH	H	OH
3	H	OH	OH	H
4	H	H	OCH ₃	OCH ₃
5	OCH ₃	H	H	OCH ₃
6	H	OC(S)N(CH ₃) ₂	H	H

We hypothesized that the new molecules inhibiting LOX have to affect the non-polar binding cavity through electronic and steric interactions, combining the structural properties of the coumarin scaffold and of an extended aromatic segment linked by an imino group.

Based on these observations, and in search of new inhibitors toward 12- and 15-LOX, fifteen coumarin derivatives were synthesized and their inhibition determined on soybean 15-lipoxygenase (15-sLOX). Their structures are given in Tables 1 and 2.

Materials and methods

Melting points were determined on a Reichert-Jung Galen III hot-plate apparatus and were not corrected. ¹H- and ¹³C-nuclear magnetic resonance (NMR) spectra were recorded on a Bruker Avance 400 spectrometer operating at 400 MHz, using the solvent or the TMS (tetramethylsilane) signal as an internal standard. The ESIMS of compounds were recorded on a Waters/Micromass Q-TOF micro high-resolution hybrid quadrupole orthogonal time-of-flight mass spectrometer with a constant nebulizer temperature of 100 °C. The experiments were carried out in positive ion mode, and the cone and extractor potentials were set at 10 and 3.0 V, respectively, with a scan range of *m/z* 100–600. The samples were directly infused into the ESI source, via a syringe pump, at flow rates of 5 μ L min⁻¹, through the instrument's injection valve. All chemical shifts are reported in the standard δ notation of parts per million.

Table 2 Derivatives of coumarins with 2-amino-2-hydroxymethyl-propane-1,3-diol

Compound	R1	R2	R3	R4
7		CH ₂ C(O)NHC(CH ₂ OH) ₃	OH	H
8		CH ₂ C(O)OCH ₂ C[(NH ₂)(CH ₂ OH) ₂]	OH	H
9	C(O)NHC(CH ₂ OH) ₃	H	OH	H
10	C(O)NHC(CH ₂ OH) ₃	H	N(C ₂ H ₅) ₂	H
11	C(O)NHC(CH ₂ OH) ₃	H	O(CH ₂) ₆ Br	H
12	C(O)NHC(CH ₂ OH) ₃	H	OCH ₃	H
13	C(O)NHC(CH ₂ OH) ₃	H	H	OH
14	C(O)NHC(CH ₂ OH) ₃	H	–CH ₂ CH ₂ NCH ₂ CH ₂ –	
15	C(O)NHC(CH ₂ OH) ₃	H	OH	OH

General procedure for the preparation of (E)-7-hydroxy-3-(benzylidenimino)-2H-chromen-2-ones 1–6

3-Amino-7-hydroxy-2H-chromen-2-one (0.56 g, 31 mmol) and the appropriate benzaldehyde (31 mmol) were dissolved in absolute EtOH (10 mL) and refluxed for 2 h. The precipitate formed was collected and washed with hot EtOH. In this way, the following (E)-7-hydroxy-3-(benzylidenimino)-2H-chromen-2-ones 1–6 were prepared (Li et al. 2009; García-Beltrán et al. 2014; García-Beltrán et al. 2012a, b; García-Beltrán et al. 2015a, b):

(E)-7-Hydroxy-3-((2-hydroxybenzylidene)amino)-2H-chromen-2-one (1)

Reaction with 2-hydroxybenzaldehyde gave 1 (0.85 g, 80 %) as a pale yellow solid, mp 248–250 °C; ¹H NMR (DMSO-d₆): δ 12.89 (s, 1H, O–H–O=C), 10.62 (br, 1H, O–H), 9.21 (s, 1H, N=CH–Ar), 8.03 (s, 1H, =C–H) 7.60 (d, 1H, Ar–H, J = 8.6 Hz), 7.55 (d, 1H, Ar–H, J = 8.6 Hz), 7.40 (dd, 1H, Ar–H, J = 8.6, 2.0 Hz), 6.96 (m, 2H, Ar–H), 6.82 (d, 1H, Ar–H, J = 8.6 Hz), 6.76 (s, 1H, Ar–H); ¹³C NMR (DMSO-d₆): δ 102.5, 112.1, 114.2, 117.2, 119.7, 119.8, 129.6, 130.4, 132.2, 132.7, 134, 153.3, 158.5, 160.8, 161.6, 164.4. HRMS: [M + Na]⁺, C₁₆H₁₁NNaO₄, found: 304.0592; calcd.: 304.0580.

(E)-3-((2,4-Dihydroxybenzylidene)amino)-7-hydroxy-2H-chromen-2-one (2)

Reaction with 2,4-dihydroxybenzaldehyde (31 mmol) gave 2 (0.91 g, 98%) as a red solid, mp > 320 °C. ¹H NMR, δ

13.36 (s, 1H, O–H–O=C), 10.57 (br, 1H, O–H), 10.37 (br, 1H, O–H), 9.02 (s, 1H, –N=CH–Ar), 7.93 (s, 1H, =C–H), 7.52 (d, 1H, J = 8.6 Hz), 7.39 (d, 1H, J = 8.6 Hz), 6.81 (dd, 1H, J = 8.0, 2.0 Hz), 6.75 (s, 1H), 6.40 (dd, 1H, J = 8.0, 2.0 Hz), 6.28 (d, 1H, J = 2.0 Hz). HRMS: [M + Na]⁺, C₁₆H₁₁NNaO₅, found: 320.0555; calcd.: 320.0535.

(E)-3-((3,4-Dihydroxybenzylidene)amino)-7-hydroxy-2H-chromen-2-one (3)

Reaction with 3,4-dihydroxybenzaldehyde (31 mmol) gave 3 as a red solid (0.93 g, 92%) mp > 320 °C. ¹H NMR (DMSO-d₆): δ 10.46 (br, 1H, O–H), 10.17 (br, 1H, O–H), 9.87 (br, 1H, O–H), 8.80 (s, 1H, –N=CH–Ar), 7.72 (s, 1H, =C–H), 7.52 (d, 1H, Ar–H, J = 8.0 Hz) 7.49 (s, 1H, Ar–H), 7.30 (d, 1H, Ar–H, J = 8.0 Hz), 6.89 (d, 1H, Ar–H, J = 8.0 Hz), 6.80 (d, 1H, Ar–H, J = 8.0 Hz), 6.74 (s, 1H, OCH₃). HRMS: [M + Na]⁺, C₁₆H₁₁NNaO₅, found: 320.0547; calcd.: 320.0535.

(E)-3-((2,3-Dimethoxybenzylidene)amino)-7-hydroxy-2H-chromen-2-one (4)

Reaction with 2,3-dimethoxybenzaldehyde (31 mmol) gave 4 as a yellow solid; (0.93 g 92 %). mp 236–238 °C; ¹H NMR (DMSO-d₆): δ 10.63 (br, 1H, O–H), 9.35 (s, 1H, N=C–Ar), 7.11 (s, 1H, =C–H), 7.66 (m, 2H, Ar–H) 7.30 (m, 3, Ar–H), 6.90 (d, 1H, Ar–H, J = 8.2 Hz), 6.84 (s, 1H, Ar–H), 6.74 (m, 1H, Ar–H), 3.92 (s, 3H, OCH₃), 3.95 (s, 3H, OCH₃). HRMS: [M + Na]⁺, C₁₈H₁₅NO₅Na, found: 348.0121; calcd.: 348.0848.

(E)-3-((2,5-Dimethoxybenzylidene)amino)-7-hydroxy-2H-chromen-2-one (**5**)

Reaction with 2,5-dimethoxybenzaldehyde (31 mmol) gave **5** (0.5 g, 89%) as a yellow solid, mp 206–208 °C. ¹H NMR (DMSO-*d*₆): δ 10.53 (br, 1H, O–H), 9.31 (s, 1H, N=C–Ar), 7.81 (s, 1H, =C–H), 7.54 (d, 1H, Ar–H, *J* = 8.2 Hz) 7.50 (s, 2H, Ar–H), 7.09 (s, 2H, Ar–H), 6.80 (d, 1H, Ar–H, *J* = 8.2 Hz), 6.74 (s, 1H, Ar–H), 3.92 (s, 3H, OCH₃), 3.84 (s, 3H, OCH₃). HRMS: [M + Na]⁺, C₁₈H₁₅NO₅Na, found: 348.1154; calcd.: 348.0848.

(E)-O-(4-(((7-hydroxy-2-oxo-2H-chromen-3-yl) imino) methine) phenyl) dimethylcarbamothioate (**6**)

3-Amino-7-hydroxy-2H-chromen-2-one (0.56 g, 31 mmol) and O-(4-formylphenyl) dimethylcarbamothioate (0.65 g, 31 mmol) gave **6** (0.85 g, 80 %) as a yellow solid, m.p. 240–242 °C; ¹H NMR (DMSO-*d*₆): δ 8.59 (s, 1H, N=C–Ar), 7.94–7.92 (d, 1H, Ar–H, *J* = 8.6 Hz), 7.78 (s, 1H, =C–H), 7.56–7.54 (d, 1H, Ar–H, *J* = 8.0 Hz), 7.22–7.20 (d, 1H, Ar–H, *J* = 8.0 Hz), 6.81 (dd, 1H, Ar–H, *J* = 8.0, 2.0 Hz), 6.75 (d, 1H, Ar–H, *J* = 2.0 Hz), 3.36 (s, 3H, N(CH₃)₂), 3.32 (s, 3H, N(CH₃)₂); ¹³C NMR (DMSO-*d*₆): δ 39.1, 43.3, 102.3, 112.4, 114.0, 123.9, 130.0, 130.1, 132.3, 132.4, 133.8, 154.0, 156.7, 158.5, 161.1, 161.8, 186.3. HRMS: [M+H]⁺, C₁₉H₁₆N₂O₄S, found: 369.0895; calcd.: 369.4143.

Synthesis of derivatives of coumarins with 2-amino-2-hydroxymethyl-propane-1,3-diol (7 and 8)

1.0 g of 2-(7-hydroxy-2-oxo-2H-chromen-4-yl) acetate (4 mmol) and 0.6 g of 2-amino-2-(hydroxymethyl) propane-1,3-diol (“tris”) (5 mmol) were dissolved in 30 mL of ethanol and the mixture was heated at reflux for 20 h (Huff et al. 1999; García-Beltrán et al. 2012a; García-Beltrán et al. 2013; Aliaga et al. 2014; Kostova and Saso 2013). The product was purified by column chromatography using as mobile phase DCM / MeOH 98:2 to obtain compound **7**: 0.9 g, white solid, 70%, mp 145–147 °C; ¹H NMR (400 MHz, DMSO-*d*₆): δ 7.65 (s, 1H), 7.62 (d, 1H, *J* = 8.6), 6.75 (dd, 1H, *J* = 8.6, 2.0), 6.69 (d, 1H, *J* = 2.0), 6.17 (s, 1H), 4.70 (br, 3H), 3.70 (s, 2H), 3.55 (s, 6H); ¹³C NMR (100 MHz, DMSO-*d*₆): δ 60.8, 62.9, 102.7, 111.7, 111.8, 113.5, 127.3, 152.1, 155.5, 160.8, 162.0, 169.2. HRMS: [M + Na]⁺, C₁₅H₁₇NNaO₇, found: 346.0897; calcd: 346.0903.

When the reaction is extended for an additional 48 h allowing the almost complete evaporation of the solvent, a mixture of compounds **7** and **8** was obtained and fractionated by column chromatography using as mobile phase DCM/MeOH 98:2, compound **8**. 0.35 g, white solid, 27%, m.p. 240–242 °C; ¹H NMR (DMSO-*d*₆): δ 10.58 (br, 1H,

O–H), 7.63 (d, 1H, Ar–H, *J* = 8.8 Hz), 6.77 (dd, 1H, Ar–H, *J* = 8.8, 2.0 Hz), 6.71 (d, 1H, Ar–H, *J* = 2.0 Hz), 6.30 (s, 1H, =C–H), 4.79 (br, 2H, –NH₂–), 4.10 (s, 2H, –CH₂–), 3.78 (s, 2H, –CH₂–), 3.43–3.30 (m, 4H, –CH₂–); ¹³C NMR (DMSO-*d*₆): δ 31.2, 64.2, 71.1, 77.2, 102.7, 111.6, 113.4, 127.2, 151.2, 155.4, 160.1, 161.7, 163.1. HRMS: [M + H]⁺, C₁₅H₁₇NNaO₇, found: 324.0972; calcd: 324.1005.

N-(1,3-Dihydroxy-2-(hydroxymethyl) propan-2-yl)-7-hydroxy-2-oxo-2H-chromene-3-carboxamide (**9**)

It is synthesized from a solution of 7-hydroxy-2-oxo-2H-1-benzopirane-3-ethyl ester (1.0 g, 4.2 mmol) and 2-amino-2-(hydroxymethyl) propane-1, 3-diol (tris) (0.517 g, 5 mmol) in 20 ml of EtOH was stirred and refluxed for 20 h. After that time a precipitate is filtered and washed with hot EtOH, yielding the compound known as light yellow (**9**). This was a return of (0.98 g, 75.5%). mp 252–254; ¹H NMR (400 MHz, DMSO-*d*₆): 8.98 (s, 1H), 8.74 (s, 1H), 7.72 (d, 1H, *J* = 8.6), 6.79 (dd, 1H, *J* = 8.6, 2.0), 6.684 (d, 1H, *J* = 2.0), 7.435 (t, 1H), 4.78 (br, 3H), 3.63 (s, 6H); ¹³C NMR (100 MHz, DMSO-*d*₆): δ 60.8, 62.7, 102.4, 110.6, 112.5, 115.9, 132.3, 148.35, 157.3, 161.88, 162.6, 166.8. HRMS: [M + Na]⁺, C₁₄H₁₅NNaO₇, found: 332.0746; calcd: 332.0746.

7-(Diethylamino)-*N*-(1,3-dihydroxy-2-(hydroxymethyl) propan-2-yl)-2-oxo-2H-chromene-3-carboxamide (**10**)

A solution of ethyl 7-(diethylamino)-2-oxo-2H-chromene-3-carboxylate (3.0 g, 10.37 mmol) and 2-amino-2-(hydroxymethyl)propane-1,3-diol (TRIS) (1.33 g, 11.0 mmol) in 30 mL of EtOH was stirred and refluxed for 20 h. The precipitate formed was filtered and washed with hot EtOH, yielding the compound (**10**) as light yellow crystals (2.83 g, 74.9%); mp 159–161 °C; ¹H NMR (400 MHz, DMSO-*d*₆): δ 9.02 (s, 1H), 8.66 (s, 1H), 7.66 (d, *J* = 8.0, 1H), 6.79 (dd, *J* = 8.6, 1.0, 1H), 6.62 (d, *J* = 1.0, 1H), 3.63 (s, 6H), 3.47 (q, *J* = 8.0, 4H), 1.13 (t, *J* = 8.0, 6H); ¹³C NMR (100 MHz, DMSO-*d*₆): δ 12.7, 44.7, 57.0, 63.0, 96.2, 108.0, 109.9, 110.5, 131.9, 148.0, 152.8, 157.7, 162.1, 162.9. HRMS: [M]⁺, C₁₈H₂₈N₂NaO₆, found: 364.9670; calcd: 364.3930.

7-((6-bromohexyl) oxy)-*N*-(1,3-dihydroxy-2-(hydroxymethyl)propan-2-yl)-2-oxo-2H-chromene-3-carboxamide (**11**)

A mixture of **9** (1.5 g, 4.8 mmol), K₂CO₃ (2.07 g, 15 mmol), and 1,6-dibromohexane (10.98 g, 45 mmol), was dissolved in DMF (100 mL). The solution was stirred for 4 h at 60 °C and then diluted with water (100 mL). An organic layer that formed was extracted with methylene chloride, and the extract was washed with water, dried, and concentrated to dryness under reduced pressure. The residue was purified by

CC using as mobile phase Hex:AcOEt, affording crystals (1.97 g, 78.8 %): mp 176–178. ^1H NMR (200 MHz, CDCl_3); δ 8.97 (s, 1H), 8.86 (s, 1H, H-4), 7.89 (d, 1H, $J = 8.0$ Hz), 7.12 (d, 1H, $J = 2.0$ Hz), 7.03 (dd, 1H, $J = 8.0, 1.0$ Hz), 4.85 (t, 2H, $J = 8.0$ Hz), 3.66 (m, 2H), 3.54 (t, 2H, $J = 8.0$), 3.35 (s, 6H), 1.78 (m, 2H), 1.45 (m, 2H). HRMS: $[\text{M} + \text{Na}]^+$, $\text{C}_{20}\text{H}_{26}\text{BrNNaO}_7$, found: 494.1125; calcd: 494.0790.

N-(1,3-dihydroxy-2-(hydroxymethyl) propan-2-yl)-7-methoxy-2-oxo-2H-chromene-3-carboxamide (**12**)

A solution of ethyl 7-methoxy-2-oxo-2H-chromene-3-carboxylate (1.0 g, 4.0 mmol) and 2-amino-2-(hydroxymethyl)propane-1,3-diol (TRIS) (0.517 g, 5 mmol) in 20 mL of EtOH was stirred and refluxed for 20 h. The precipitate formed was filtered and washed with hot EtOH, yielding the compound (**12**) as white solid (0.95 g, 70 %); mp 139–141 °C; ^1H NMR (400 MHz, DMSO-d_6): δ 8.98 (s, 1H), 8.84 (s, 1H), 7.88 (d, $J = 8.0$, 1H), 7.11 (d, $J = 1.0$, 1H), 7.03 (dd, $J = 8.0, 1.0$, 1H), 4.85 (t, $J = 8.0$, 3H), 3.89 (s, 3H), 3.68 (m, $J = 8.0$, 6H); ^{13}C NMR (100 MHz, DMSO-d_6): δ 56.6, 60.6, 62.7, 100.6, 112.4, 114.1, 115.3, 131.9, 148.2, 156.6, 161.4, 161.8, 164.8. HRMS: $[\text{M} + \text{Na}]^+$, $\text{C}_{15}\text{H}_{17}\text{NNaO}_7$, found: 346.1005; calcd: 346.0903.

N-(1,3-dihydroxy-2-(hydroxymethyl) propan-2-yl)-8-hydroxy-2-oxo-2H-chromene-3-carboxamide (**13**)

A solution of ethyl 8-hydroxy-2-oxo-2H-chromene-3-carboxylate (1.0 g 4.2 mmol) and 2-amino-2-(hydroxymethyl)propane-1,3-diol (TRIS) (0.517 g, 5 mmol) in 20 mL of EtOH was stirred and refluxed for 20 h. The precipitate formed was filtered and washed with hot EtOH, yielding the compound (**13**) as whitish solid (0.95 g, 70 %); mp 245–247 °C; ^1H NMR (400 MHz, DMSO-d_6): δ 9.07 (s, 1H), 8.67 (s, 1H), 7.30 (m, 1H), 7.20 (m, 2H), 3.63 (s, 6H); ^{13}C NMR (100 MHz, DMSO-d_6): δ 63.9, 69.2, 112.1, 117.5, 118.2, 121.2, 122.9, 127.5, 143.9, 144.7, 160.1, 162.7. HRMS: $[\text{M} + \text{Na}]^+$, $\text{C}_{14}\text{H}_{15}\text{NNaO}_7$, found: 332.0755; calcd: 332.0746.

N-(1,3-dihydroxy-2-(hydroxymethyl) propan-2-yl)-11-oxo-2,3,5,6,7,11-hexahydro-1H-pyrano[2,3-f]pyrido[3,2,1-ij]quinoline-10-carboxamide (**14**)

A solution of ethyl 11-oxo-2,3,5,6,7,11-hexahydro-1H-pyrano[2,3-f]pyrido[3,2,1-ij]quinoline-10-carboxylate (1.0 g, 3.2 mmol) and 2-amino-2-(hydroxymethyl)propane-1,3-diol (TRIS) (0.48 g, 4.0 mmol) in 20 mL of EtOH was stirred and refluxed for 20 h. The precipitate formed was filtered and washed with hot EtOH, yielding the compound

(**14**) as yellow solid (1.1 g, 78.1 %); mp 172–174 °C; ^1H NMR (400 MHz, DMSO-d_6): δ 7.98 (s, 1H), 6.56 (s, 1H), 4.79 (s, 3H), 3.55 (s, 6H), 3.14 (s, 4H), 2.46 (s, 6H), 1.08 (s, 4H); ^{13}C NMR (100 MHz, DMSO-d_6): δ 20.6, 21.4, 22.4, 27.3, 49.5, 49.8, 61.8, 64.8, 106.5, 107.8, 111.3, 129.7, 147.2, 160.3, 167.9. HRMS: $[\text{M} + \text{Na}]^+$, $\text{C}_{20}\text{H}_{24}\text{N}_2\text{NaO}_6$, found: 411.1552; calcd: 411.1532.

N-(1,3-dihydroxy-2-(hydroxymethyl) propan-2-yl)-7,8-dihydroxy-2-oxo-2H-chromene-3-carboxamide (**15**)

A solution of ethyl 7,8-dihydroxy-2-oxo-2H-chromene-3-carboxylate (0.75 g, 3.0 mmol) and 2-amino-2-(hydroxymethyl)propane-1,3-diol (TRIS) (0.4 g, 4.0 mmol) in 20 mL of EtOH was stirred and refluxed for 20 h. The precipitate formed was filtered and washed with hot EtOH, yielding the compound (**15**) as light yellow solid (0.92 g, 94.4 %); mp 274–276 °C; ^1H NMR (400 MHz, DMSO-d_6): δ 9.14 (s, 1H), 8.50 (s, 1H), 7.09 (d, $J = 8.0$, 1H), 6.55 (d, $J = 8.0$, 1H), 3.62 (s, 6H); ^{13}C NMR (100 MHz, DMSO-d_6): δ 60.2, 60.9, 61.1, 62.6, 106.8, 108.4, 116.2, 123.4, 133.7, 142.7, 148.2, 162.7, 164.2, 164.6. HRMS: $[\text{M} + \text{Na}]^+$, $\text{C}_{14}\text{H}_{15}\text{NNaO}_8$, found: 411.1552; calcd: 411.1532.

Kinetics and IC_{50} assay

All compounds were screened for activity as soybean 15-lipoxygenase (15-sLOX) inhibitors. In all cases the preliminary evaluation was done at 1 $\mu\text{mol/mL}$. The inhibition of enzyme activity was determined following the formation of the conjugated diene product at 234 nm ($\epsilon = 25,000 \text{ M}^{-1}\text{cm}^{-1}$) using a Perkin-Elmer Lambda 25 UV/Vis spectrophotometer, relative to control rates measured for the carrier solvent DMSO, as previously published. All reactions were done in a volume of 2 mL constantly stirred using a magnetic stir bar at room temperature (23 °C). The 15-sLOX specific activity was 100,000 U/mg, (Cayman Chemical Catalog Number 60712). Reactions were carried out in 25 mM HEPES (pH 7.4), 0.01% Triton X-100 and 10 μM AA. The concentration of AA was quantitatively determined by allowing the enzymatic reaction to reach completion. IC_{50} values were obtained by determining the enzymatic rate at various inhibitor concentrations and plotted against inhibitor concentration, followed by a hyperbolic saturation curve fit. The data used for the saturation curves were obtained in duplicate or triplicate, depending on their quality. Additionally, the K_i and inhibitor behavior of the most potent compound (**6**) was determined against 15-sLOX (Holman et al. 1998; Deschamps et al. 2007; Carroll et al. 2001; Weckler et al. 2009a, b).

Pseudoperoxidase activity assay

The reductive properties of the compounds were determined by monitoring the pseudo-peroxidase activity of 15-sLOX in the presence of the inhibitor and 13-HPODE. Activity was characterized by direct measurement of the product degradation following the decrease of absorbance at 234 nm using a Perkin-Elmer Lambda 25 UV/Vis spectrometer (25 mM HEPES (pH 7.4), 0.01% Triton X-100, and 10 μ M 13-HPODE). All reactions were performed in 2 mL of buffer with constant magnetic stirring (22 °C) (Riendeau et al. 1991; Hoobler et al. 2013).

Reaction was initiated by addition of 10 μ M inhibitor (1:1 ratio to product), and a positive result for activity reflected a loss of more than 40% of product absorption using nordihydroguaiaretic acid (NDGA), a known reductive inhibitor. Individual controls were conducted with inhibitor alone with product and enzyme alone with product. These negative controls formed the baseline for the assay, reflecting non-pseudoperoxidase dependent hydroperoxide product decomposition. To rule out the auto-inactivation of the enzyme from pseudo-peroxidase cycling, 15-sLOX residual activities were measured after the assay was complete, 20 μ M AA was added to the reaction mixture and the residual activity was determined by comparing the initial rates with inhibitor and 13-(S)-HPODE vs. inhibitor alone, since the inhibitor by itself inherently lowers the rate of the oxygenation. Activity is characterized by direct measurement of the product formation with the increase of absorbance at 234 nm.

Evaluation of radical-trapping activity using DPPH

The DPPH scavenging capacity assay was performed using 20 μ L of different compound concentrations in methanol, which were added to 1 mL of 0.1 mM DPPH in methanol. Each mixture was vortexed for a few seconds and stirred in the dark for 30 min at room temperature. The absorbance (A) of each reaction mixture was measured at 517 nm against a blank of methanol using a UV–visible spectrometer (Perkin-Elmer 25). The scavenging capacity of each sample was calculated on the basis of an ascorbic acid standard curve. Duplicate reactions were carried out with each sample. The correlation among the IC₅₀ values for enzyme inhibition and the scavenger properties of the compounds was evaluated using a correlation matrix including the IC₅₀ for enzyme inhibition of twelve compounds and the percentage of remaining DPPH radical for three independent experiments with each enzyme. The Pearson correlation for the IC₅₀ and % remaining DPPH was done using GraphPad Prism v.5 DEMO for windows, considering an alpha value of 0.05 (Miliauskas et al. 2004; GraphPad Software).

Computational studies

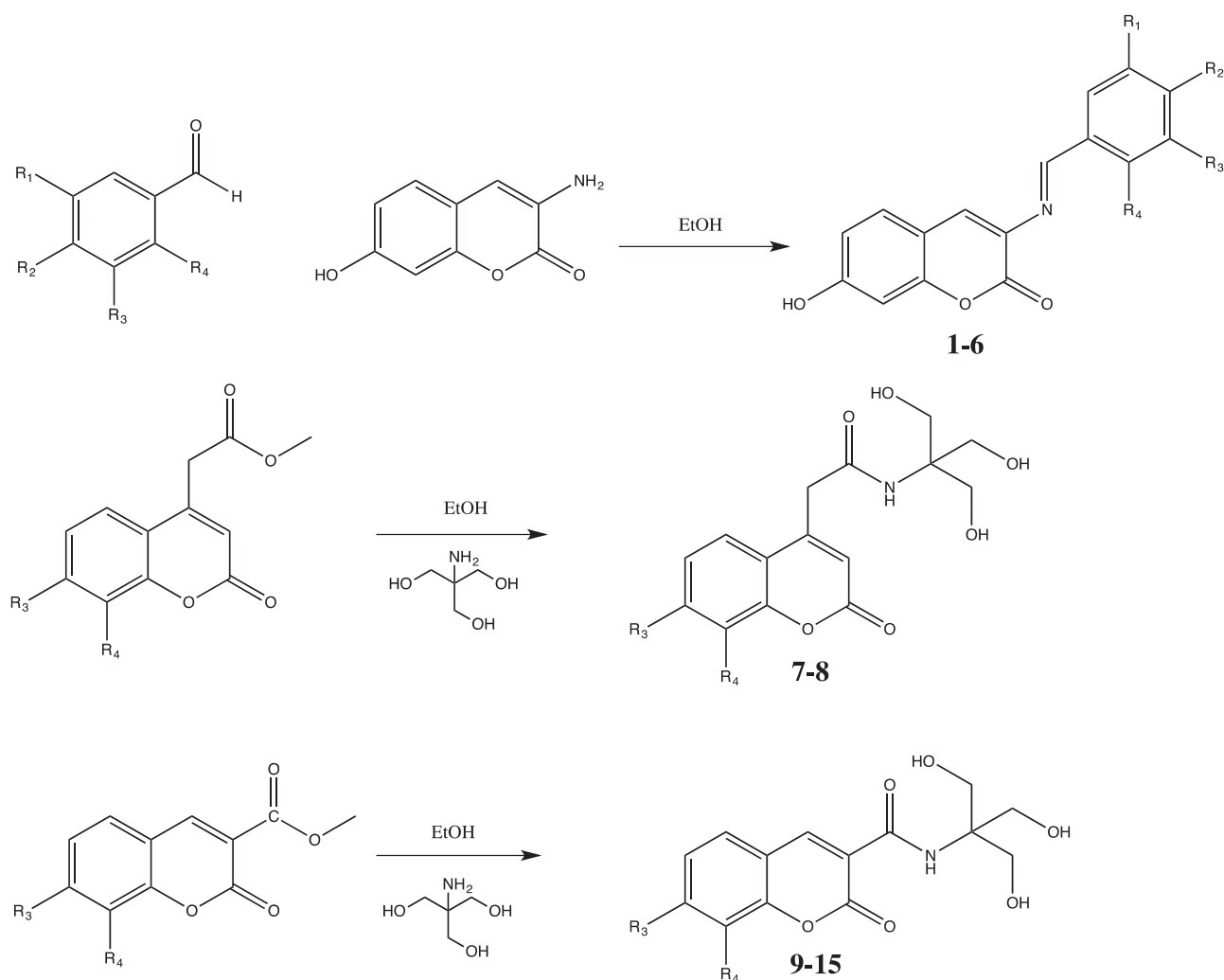
The structures of ligands were built using GaussView 5.0 software. The Chelpg charges were obtained at the B3LYP/6-31G** level of theory, employing the Gaussian 09 package. Docking studies of **3**, **5**, **6**, **7** and NDGA into the active site of the crystal structures of 15-sLOX (PDB ID: 1N8Q) (Borbulevych et al. 2004), human 5-LOX (PDB ID: 3O8Y) (Gilbert et al. 2011), human 12-S-LOX (PDB ID: 3D3L) (Tresaugues et al. 2008), rabbit 15-LOX-1 (PDB ID: 2P0M) (Choi et al. 2008) and human 15-LOX-2 (PDB ID: 4NRE) (Kobe et al. 2014) were done using the Lamarckian algorithm in AutoDock 4.2 (Morris et al. 1996) and assuming total flexibility of the inhibitors and partial flexibility of the His residues coordinated to Fe(III) inside the binding site. The grid maps were built with 60 \times 60 \times 60 points, with a grid-point spacing of 0.375 Å. The AutoTors option was used to define the ligand torsions, and the docking results were then analyzed by a ranked cluster analysis, resulting in conformations with the highest overall binding energy (lowest $\Delta G_{\text{binding}}$ value). When the complexes for **6** and NDGA had been obtained, the whole systems were inserted into a water box (TIP3) and ions were added creating an overall neutral system using NaCl. The ions were equally distributed in the water box. The final systems contained approximately 35,000 atoms and were submitted to a molecular dynamics (MD) simulation for 10 ns using NAMD 2.6 (Phillips et al. 2005).

The NPT ensemble was used to perform MD calculations. Periodic boundary conditions were applied to the system in the three coordinate directions. A pressure of 1 atm. and a temperature of 310 K were maintained.

Results and discussion

Compounds **1–6** were synthesized starting from 2, 4-dihydroxybenzaldehyde, which was subsequently condensed with acetylglycine (Knoevenagel) and hydrolyzed in one step to afford 3-amino-7-hydroxycoumarin (SI). The coumarins were condensed with appropriately substituted benzaldehydes to obtain compounds **1–6** (Li et al. 2009; García-Beltrán et al. 2014; García-Beltrán et al. 2012a, b, 2015a, b), in yields higher than 90%. Finally, compounds **7–15** were synthesized according to literature protocols (Scheme 1) (Huff et al. 1999; García-Beltrán et al. 2012a; García-Beltrán et al. 2013; Aliaga et al. 2014; Kostova and Saso 2013).

A preliminary screen was carried out (Holman et al. 1998; Deschamps et al. 2007; Carroll et al. 2001; Wecksler et al. 2009a, b), for all prepared compounds against 15-sLOX. The soybean (15-sLOX) enzyme was taken as a study model because, although the human enzyme is also



Scheme 1 Synthesis of (*E*)-3-(benzylideneamino)-7-hydroxy-2*H*-chromen-2-one and 2-amino-2-hydroxymethylpropane-1,3-diol derivatives

commercially available, it is less stable than that of plant origin, besides exhibiting low biological activity in *in vitro* studies. An alignment of the sequences of human and soybean LOX yielded a 28% identity. Although this could be taken as an indication of little identity between the two isoforms, a comparative study of their active sites showed that all residues that are part of the binding site, and that interact with the AA and iron (Wecksler et al. 2009a), are highly conserved in both systems. Thus, we can consider 15-sLOX as a first good model for studying the mechanisms of inhibition of 12- or 15-LOX, an assumption that was supported by docking studies.

This preliminary screen was expected to reveal potentially active inhibitors of the human enzyme. The percentages of inhibition assayed at 1 μ M concentration of the coumarin derivatives are displayed in Table 3.

This preliminary screening singled out coumarins **3**, **5**, **6**, and **7** as the most promising derivatives, with percentage inhibition near or higher than 50%. IC_{50} values for these

molecules were then determined at different inhibitor concentrations. Two of them (**3** and **6**) proved effective at a submicromolar, and the other two (**5** and **7**) at a micromolar concentration. With the aid of the Cheng-Prusoff Eq. (1) (Cheng and Prusoff 1973) the corresponding inhibition constants K_i for these derivatives were calculated.

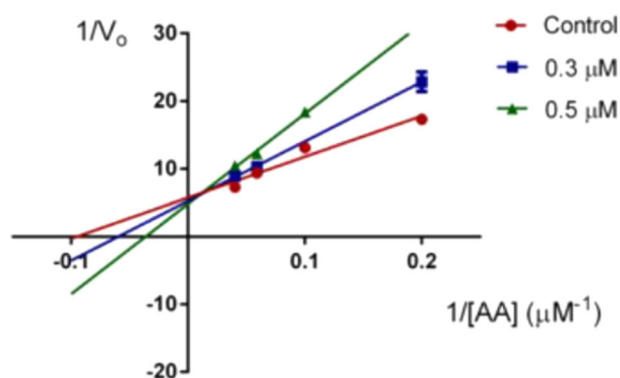
$$K_i = \frac{IC_{50}}{1 + \frac{[S]}{K_m}} \quad (1)$$

Table 3 lists the IC_{50} and the K_i values for coumarin derivatives **3**, **5**, **6**, and **7**. For the sake of comparison, the corresponding values for 7-hydroxy-8-methyl-3-phenyl-4*H*-chromen-4-one (IR-204) and for the potent competitive inhibitor nordihydroguaiaretic acid (NDGA) were also included.

To determine the type of inhibition of these compounds, kinetic studies were carried out the Fig. 1 reproduces Lineweaver-Burk plots for the most promising inhibitor **6**, in an indication of a competitive behavior for this molecule.

Table 3 Biological results of the most promising inhibitors against 15-sLOX

Compound	Percentage of Inhibition (\pm) SD	IC ₅₀ (μ M) (\pm) SD	K _i (μ M)	Pseudoperoxidase activity	% DPPH
1	33 \pm 0.20				
2	10 \pm 1.10				
3	60 \pm 0.30	0.37 \pm 0.00	0.18	+	93.7
4	4 \pm 0.10				
5	48 \pm 2.80	1.49 \pm 0.06	0.76	+	71.3
6	65 \pm 4.70	0.34 \pm 0.02	0.17	+	81.1
7	36 \pm 1.70	5.13 \pm 0.37	2.63	+	21.9
8	19 \pm 1.10				
9	16 \pm 1.20				
10	13 \pm 2.20				
11	19 \pm 6.00				
12	11 \pm 3.70				
13	12 \pm 1.40				
14	24 \pm 2.50				
15	18 \pm 1.50				
NDGA ^a		1.13 \pm 0.02	0.29	+	N.D
IR204 ^b		>100	>100	-	N.D

^a Nordihydroguaiaretic acid^b 7-hydroxy-8-methyl-3-phenyl-4H-chromen-4-one**Fig. 1** Biological activity of compound **6** and Lineweaver–Burk plot of compound **6** in front of 15-sLOX

A possible correlation between the inhibitory activities of **3**, **5**, **6**, and **7** and their pseudo-peroxidase and antioxidant activities was next investigated (Table 3). It is seen that all tested inhibitors exhibited pseudoperoxidase activity (Riendeau et al. 1991; Hoobler et al. 2013), suggesting that the coumarin derivatives affect the oxidation state of iron in the active site, reducing it from ferric (active) to ferrous (inactive). Additionally, the four derivatives were capable of bleaching DPPH (Miliauskas et al. 2004; GraphPad Software), and the percentage bleaching varied inversely with their inhibitory constants K_i , suggesting that the

effectiveness of these 15-sLOX inhibitors could be ascribed to their antioxidant activities.

An important result of Table 3, is that two of the new coumarin derivatives (compounds **3** and **6**) showed comparable and even better activities than the potent REDOX inhibitor NDGA with a $K_i = 0.29 \mu\text{M}$ (Somvanshi et al. 2008). Our kinetic studies revealed that **6** compete with the substrate for the binding site of the enzyme, in the same way as NDGA.

On the other hand, steric effects apparently play an important role in the interaction with the binding site as we observed in compounds **5** and **7** which showed the worst results of IC₅₀ (5.13 and 1.49 μM respectively), particular the compound **7**, had the lowest percentage of DPPH bleaching seen in this series, despite that above, this results explain the different chemical interaction responsible for LOX inhibition and that the presences of catechol or hydroxyl group not guaranteed the potency of drugs.

In order to gain some insight into the structural factors responsible for the inhibitory activity of the coumarin derivatives, docking studies of these molecules and NDGA into the active site of 15-sLOX were carried out (Gauss-View, Version 5; Frisch et al. 2009; Berman et al. 2000; Morris et al. 1996; Phillips et al. 2005). Starting from the known structure of crystalline 15-sLOX (PDB ID: 1N8Q) (Borbulevych et al. 2004), docking studies revealed a variety of interactions of this molecule with polar and non-polar amino acids.

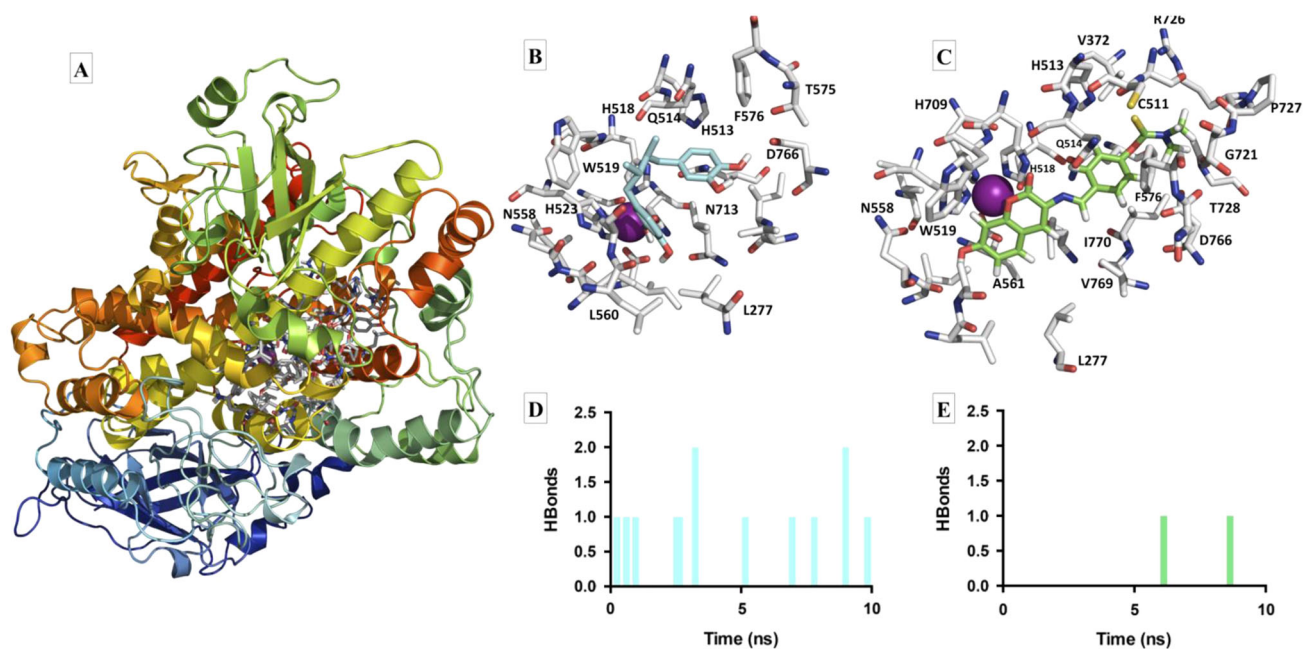


Fig. 2 **a** Representation of LOX **b** and **c** shows the main interactions of NDGA and **6** respectively inside the binding cavity. The hydrogen bonds generated during the simulation are displayed in **(d)** NDGA and **e** compound **6**

Studies with the best LOX inhibitor revealed a relevant π -cation interaction between the chromene ring and the iron cation located in the binding site. The presence of the catechol group in compound **3** also favored the inhibition, a result that can be related with the antioxidant and pseudo-peroxidase activities shown in Table 3, common to other good inhibitors assayed in our group (Mascayano et al. 2013, 2015).

The docking results with compound **6** showed that the dimethylcarbamothioate substituent is located near the basic residue R726, favoring a strong interaction between ligand and protein through the sulphur atom (Fig. 2c). Compound **6** is located close (≈ 4 Å) to Fe(III) and $\Delta G_{\text{binding}}$ of -5.85 Kcal/mol and exhibits strong interactions with Q514, H518, W519, H523 and R726. Among these residues, Q514 plays a decisive role in promoting the binding of fatty acids into the catalytic site. By coordinating with H518, it draws the central ring of **6** close to the metal, through interactions with its imine group. Docking of **6** against other isoforms of LOX reveals a lower affinity in the human crystal structure of 5-LOX (-0.38 Kcal/mol), while for human 12-S-LOX and 15-LOX-2, affinities (-11.09 and -5.47 Kcal/mol respectively) were comparable or better than for 15-sLOX. Comparison of binding energies from docking studies with human 15-LOX-1 shows similar values to those with 15-sLOX (used in this study). It is important to mention that in all cases the ligands interact in a similar way in the LOX cavity, positioning the imine group near the iron cation (≈ 3 Å).

Compounds **3**, **5**, and **7** (IC_{50} 0.37, 1.49, and 5.13 μM respectively) were next docked into the binding site of 15-sLOX. The results showed that for compounds **6**, **5**, and **3**, the imine group was located close to the iron ion. This was not observed for compound **7**, which had the 2-amino-2-hydroxymethyl-propane-1,3-diol substituent positioned near the metal. A good relationship was found between the binding energies and the activities of compounds **6** and **7** ($\Delta G_{\text{binding}} = -5.85$ and -1.89 Kcal/mol), the most and least active, respectively. Docking thus provided a preliminary approximation and insight into the protein–ligand interactions in the enzyme cavity.

The complex LOX-**6** was studied using MD simulations in order to rationalize the system from a dynamic and energetic point of view. (Fig. 2c). Is important to mention that Q514, which has been described an important residue that aid to the fatty acid to binding into the catalytic site is in coordination with H518 along the MD helping to maintain the central ring of **6** close to the metal due to the electrostatic interaction formed with imine group.

As was mentioned above, NDGA is a REDOX inhibitor of LOX. In order to evaluate the specific interactions between NDGA and the protein computational studies were carried out. The docking results ($\Delta G_{\text{binding}} -6.42$ Kcal/mol) showed that the presence of the catechol group is fundamental for their interaction with iron (1.7 Å), but the hydrophobicity of pocket is also relevant, residues as F, V, I and W allow the correct positioning of ligand into the

binding site gave as result the loss of the activity of the enzyme.

The analysis of LOX-NDGA complex by MD showed a strong interaction between the catechol group and the iron cation. This would validate the suggestion from kinetic studies that inhibition by NDGA occurs by hydrogen transfer to iron (Somvanshi et al. 2008) in the similar way that coumarin **6**, in both cases the REDOX mechanisms were the responsible. In addition, NDGA established more hydrogen bonds with surrounding residues than **6** (Fig. 2d, e).

Conclusion

In conclusion, among the newly studied coumarins, **3**, **5**, **6**, and **7** all of them showed promising inhibitory activities against 15-LOX. The most powerful inhibitor, **6** (IC_{50} 0.34 μ M), proved even more potent than NDGA (IC_{50} 1.13 μ M). Kinetic measurements suggested a competitive mechanism (K_i 0.17 μ M) for its action, in agreement with its excellent REDOX and pseudoperoxidase activities. Molecular simulation studies supported these observations and revealed that binding inside the active site occurs mainly through van der Waals and electrostatic interactions.

Acknowledgements Financial support from DICYT 021641MC; Fondecyt 1120379, Fondecyt 1161375 and the Millennium Scientific Initiative (Grant P05-001-F).

Compliance with ethical standards

Conflict of interest The authors declare that they have no competing interests.

References

- Aliaga ME, Tiznado W, Cassels BK, Nunez MT, Millán D, Pérez EG, García-Beltrán O, Pavez P (2014) Substituent effects on reactivity of 3-cinnamoylcoumarins with thiols of biological interest. *RSC Adv* 4:697–704
- Armstrong MM, Diaz G, Kenyon V, Holman TR (2014) Inhibitory and mechanistic investigations of oxo-lipids with human lipoxigenase isozymes. *Bioorg Med Chem* 22:4293–4297
- Bansal Y, Sethi P, Bansal G (2013) Coumarin: a potential nucleus for anti-inflammatory molecules. *Med Chem Res* 22:3049–3060
- Bell RL, Young PR, Albert D, Lanni C, Summers JB, Brooks DW, Rubin P, Carter GW (1992) The discovery and development of zileuton: an orally active 5-lipoxygenase inhibitor. *Int J Immunopharmacol* 14:505–510
- Berman J, Westbrook Z, Feng G, Gilliland TN, Bhat H, Weissig IN, Shindyalov PE (2000) The protein data bank. *Nucleic Acids Res* 28:235–242
- Borbulevych OY, Jankun J, Selman SH, Skrzypczak-Jankun E (2004) Lipoxigenase interactions with natural flavonoid, quercetin, reveal a complex with protocatechuic acid in its X-ray structure at 2.1 Å resolution. *Proteins* 54:13–19
- Brash AR, Schneider C, Hamberg M (2012) Applications of stereospecifically-labeled fatty acids in oxygenase and desaturase biochemistry. *Lipids* 47:101–116
- Carroll J, Jonsson EN, Ebel R, Hartman MS, Holman TR, Crews P (2001) Probing sponge-derived terpenoids for human 15-lipoxygenase inhibitors. *JOC* 66:6847–6851
- Chauhan BF, Ducharme FM (2012) Anti-leukotriene agents compared to inhaled corticosteroids in the management of recurrent and/or chronic asthma in adults and children. *The Cochrane Library*
- Cheng Y, Prusoff WH (1973) Relationship between the inhibition constant (K_i) and the concentration of inhibitor which causes 50% inhibition (I_{50}) of an enzymatic reaction. *Biochem Pharmacol* 22:3099–3108
- Choi J, Chon JK, Kim S, Shin W (2008) Conformational flexibility in mammalian 15S-lipoxygenase: reinterpretation of the crystallographic data. *Proteins* 70(3):1023–1032
- Deschamps JD, Gautschi JT, Whitman S, Johnson TA, Gassner NC, Crews P, Holman TR (2007) Discovery of platelet-type 12-human lipoxigenase selective inhibitors by high-throughput screening of structurally diverse libraries. *Bioorg Med Chem* 15:6900–6908
- Frisch MJ, Trucks GW, Schlegel HB, Scuseria GE, Robb MA, Cheeseman JR, Scalmani G, Barone V, Mennucci B, Petersson GA, Nakatsuji H, Caricato M, Li X, Hratchian HP, Izmaylov AF, Bloino J, Zheng G, Sonnenberg JL, Hada M, Ehara M, Toyota K, Fukuda R, Hasegawa J, Ishida M, Nakajima T, Honda Y, Kitao O, Nakai H, Vreven T, Montgomery JA, Jr., Peralta JE, Ogliaro F, Bearpark M, Heyd JJ, Brothers E, Kudin KN, Staroverov VN, Kobayashi R, Normand J, Raghavachari K, Rendell A, Burant JC, Iyengar SS, Tomasi J, Cossi M, Rega N, Millam JM, Klene M, Knox JE, Cross JB, Bakken V, Adamo C, Jaramillo J, Gomperts R, Stratmann RE, Yazyev O, Austin AJ, Cammi R, Pomelli C, Ochterski JW, Martin RL, Morokuma K, Zakrzewski VG, Voth GA, Salvador P, Dannenberg JJ, Dapprich S, Daniels AD, Farkas Ö, Foresman JB, Ortiz JV, Cioslowski J, Fox DJ (2009) Gaussian '09, Revision A.1. '09. Wallingford, CT
- García-Beltrán O, Cassels BK, Pérez C, Mena N, Núñez MT, Martínez NP, Aliaga ME (2014) Coumarin-based fluorescent probes for dual recognition of copper (II) and iron (III) ions and their application in bio-imaging. *Sensors* 14:1358–1371
- García-Beltrán O, Mena N, Berríos TA, Castro EA, Cassels BK, Núñez MT, Aliaga ME (2012a) A selective fluorescent probe for the detection of mercury (II) in aqueous media and its applications in living cells. *Tetrahedron Lett* 53:6598–6601
- García-Beltrán O, Mena N, Friedrich LC, Netto-Ferreira JC, Vargas V, Quina FH, Cassels BK (2012b) Design and synthesis of a new coumarin-based 'turn-on' fluorescent probe selective for Cu²⁺. *Tetrahedron Lett* 2012(53):5280–5283
- García-Beltrán O, Mena N, Yañez O, Caballero J, Vargas V, Núñez MT, Cassels BK (2013) Design, synthesis and cellular dynamics studies in membranes of a new coumarin-based "turn-off" fluorescent probe selective for Fe²⁺. *Eur J Med Chem* 67:60–63
- García-Beltrán O, Rodríguez A, Trujillo A, Cañete A, Aguirre P, Gallego-Quintero S, Aliaga ME (2015a) Synthesis and characterization of a novel fluorescent and colorimetric probe for the detection of mercury (II) even in the presence of relevant biothiols. *Tetrahedron Lett* 56:5761–5766
- García-Beltrán O, Rodríguez A, Trujillo A, Cañete A, Aguirre P, Gallego-Quintero S, Aliaga ME (2015b) Synthesis and characterization of a novel fluorescent and colorimetric probe for the detection of mercury (II) even in the presence of relevant biothiols. *Tetrahedron Lett* 56:5761–5766
- Dennington R, Keith T, Millam J (2009) GaussView, Version 5 Semichem Inc., Shawnee Mission, KS,
- Giannopoulos PF, Joshi YB, Chu J, Praticò D (2013) The 12-15-lipoxygenase is a modulator of Alzheimer's-related tau pathology in vivo. *Aging Cell* 12:1082–1090

- Gilbert NC, Bartlett SG, Waight MT, Neau DB, Boeglin WE, Brash AR, Newcomer ME (2011) The structure of human 5-lipoxygenase. *Science* 331:217–219
- Gillmor SA, Villaseñor A, Fletterick R, Sigal E, Browner MF (1997) The structure of mammalian 15-lipoxygenase reveals similarity to the lipases and the determinants of substrate specificity. *Nat Struct Mol Biol* 4:1003–1009
- GraphPad Software, La Jolla California USA, www.graphpad.com
- Hadjipavlou-Litina DJ, Litinas KE, Kontogiorgis C (2007) The anti-inflammatory effect of coumarin and its derivatives. *Anti-Inflamm Anti-Allergy Agents Med Chem* 6:293–306
- Holman TR, Zhou J, Solomon EI (1998) Spectroscopic and functional characterization of a ligand coordination mutant of soybean lipoxygenase-1: first coordination sphere analogue of human 15-lipoxygenase. *JACS* 120:12564–12572
- Hoobler EK, Holz C, Holman TR (2013) Pseudoperoxidase investigations of hydroperoxides and inhibitors with human lipoxygenases. *Bioorg Med Chem* 21:3894–3899
- Hoult JRS, Paya M (1996) Pharmacological and biochemical actions of simple coumarins: natural products with therapeutic potential. *Gener Pharmacol* 27:713–722
- Huff JB, Merchant BT, Mullen CR, Venkata SRT (1999) U.S. Patent No. 5,998,593. Washington, DC: U.S. Patent and Trademark Office
- Ivanov I, Heydeck D, Hofheinz K, Roffeis J, O'Donnell VB, Kuhn H, Walther M (2010) Molecular enzymology of lipoxygenases. *Arch Biochem Biophys* 503:161–174
- Klil-Drori AJ, Ariel A (2013) 15-Lipoxygenases in cancer: a double-edged sword? *Prostaglandins Other Lipid Mediat* 106:16–22
- Kobe MJ, Neau DB, Mitchell CE, Bartlett SG, Newcomer ME (2014) The structure of human 15-lipoxygenase-2 with a substrate mimic. *J Biol Chem* 289(12):8562–8569
- Kostova I, Saso L (2013) Advances in research of Schiff-base metal complexes as potent antioxidants. *Curr Med Chem* 20:4609–4632
- Kotali A, Nasiopoulou DA, Tsoleridis CA, Harris PA, Kontogiorgis CA, Hadjipavlou-Litina DJ (2016) Antioxidant Activity of 3-[N-(Acylhydrazono) ethyl]-4-hydroxy-coumarins. *Molecules* 21:138
- Krönke G, Katzenbeisser J, Uderhardt S, Zaiss MM, Scholtyssek C, Schabbauer G, Baenckler HW (2009) 12/15-lipoxygenase counteracts inflammation and tissue damage in arthritis. *J Immunol* 183:3383–3389
- Kulkarni S, Das S, Funk CD, Murray D, Cho W (2002) Molecular basis of the specific subcellular localization of the C2-like domain of 5-lipoxygenase. *J Biol Chem* 277:13167–13174
- Li HY, Gao S, Xi Z (2009) A colorimetric and “turn-on” fluorescent chemosensor for Zn (II) based on coumarin Schiff-base derivative. *Inorg Chem Commun* 12:300–303
- Mascayano C, Espinosa V, Sepúlveda-Boza S, Hoobler EK, Pery S (2013) In Vitro study of isoflavones and isoflavans as potent inhibitors of human 12-and 15-lipoxygenases. *Chem Biol Drug Des* 82:317–325
- Mascayano C, Espinosa V, Sepúlveda-Boza S, Hoobler EK, Pery S, Diaz G, Holman TR (2015) Enzymatic Studies of Isoflavonoids as Selective and Potent Inhibitors of Human Leukocyte 5-Lipoxygenase. *Chem Biol Drug Des* 86:114–121
- Miliauskas G, Venskutonis PR, Van Beek TA (2004) Screening of radical scavenging activity of some medicinal and aromatic plant extracts. *Food Chem* 85:231–237
- Morris GM, Goodsell DS, Huey R, Olson AJ (1996) Distributed automated docking of flexible ligands to proteins: parallel applications of AutoDock 2.4. *Comput Aided Mol Des* 10:293–304
- Needleman P, Jakschik BA, Morrison AR, Lefkowitz JB (1986) Arachidonic acid metabolism. *Annu Rev Biochem* 55:69–102
- Newcomer ME, Brash AR (2015) The structural basis for specificity in lipoxygenase catalysis. *Protein Sci* 24:298–309
- Oldham ML, Brash AR, Newcomer ME (2005) Insights from the X-ray Crystal Structure of Coral 8R-Lipoxygenase calcium activation via a c2-like domain and a structural basis of product chirality. *J Biol Chem* 280:39545–39552
- Phillips JC, Braun R, Wang W, Gumbart J, Tajkhorshid E, Villa E, Schulten K (2005) Scalable molecular dynamics with NAMD. *J Comput Chem* 26:1781–1802
- Ribeiro D, Freitas M, Tomé SM, Silva AM, Porto G, Cabrita EJ, Marques MM, Fernandes E (2014) Inhibition of LOX by flavonoids: a structure–activity relationship study. *Eur J Med Chem* 72:137–145
- Riendeau D, Falgueyret JP, Guay J, Ueda N, Yamamoto S (1991) Pseudoperoxidase activity of 5-lipoxygenase stimulated by potent benzofuranol and N-hydroxyurea inhibitors of the lipoxygenase reaction. *Biochem J* 274:287–292
- Sarveswaran S, Chakraborty D, Chitale D, Sears R, Ghosh J (2015) Inhibition of 5-lipoxygenase selectively triggers disruption of c-Myc signaling in prostate cancer cells. *J Biol Chem* 290:4994–5006
- Da Silva CM, Da Silva DL, Modolo LV, Alves RV, De Resende MA, CVB Martins, De Fátima A (2011) Schiff bases: a short review of their antimicrobial activities. *J Adv Res* 2:1–8
- Singh D, Pathak DP (2016) Coumarins: an overview of medicinal chemistry. Potential for new drug molecules. *Int J Pharm Sci Rev Res* 7:482
- Skrzypczak-Jankun E, Zhou K, McCabe NP, Selman SH, Jankun J (2003) Structure of curcumin in complex with lipoxygenase and its significance in cancer. *Int J Mol Med* 12:17–24
- Somvanshi RK, Singh AK, Saxena M, Mishra B, Dey S (2008) Development of novel peptide inhibitor of Lipoxygenase based on biochemical and BIAcore evidences. *BBA Proteins Proteom* 1784:1812–1817
- Srivastava P, Vyas VK, Variya B, Patel P, Qureshi G, Ghate M (2016) Synthesis, anti-inflammatory, analgesic, 5-lipoxygenase (5-LOX) inhibition activities, and molecular docking study of 7-substituted coumarin derivatives. *Bioorg Chem* 67:130–138
- Tomchick DR, Phan P, Cymborowski M, Minor W, Holman TR (2001) Structural and functional characterization of second-coordination sphere mutants of soybean lipoxygenase-1. *Biochemistry* 40:7509–7517
- Torres R, Mascayano C, Nunez C, Modak B, Faini F (2013) Coumarins Of *Haplopappus multifolius* and derivative as inhibitors of LOX: evaluation in-vitro and docking studies. *J Chil Chem Soc* 58:2027–2030
- Tresaugues L, Moche M, Arrowsmith CH, Berglund H, Busam RD, Collins R, Graslund, S (2008) Crystal structure of the lipoxygenase domain of human Arachidonate 12-lipoxygenase, 12S-type. Submitted. PDB entry 3D3L
- Weckslar AT, Garcia NK, Holman TR (2009a) Substrate specificity effects of lipoxygenase products and inhibitors on soybean lipoxygenase-1. *Bioorg Med Chem* 17:6534–6539
- Weckslar AT, Kenyon V, Garcia NK, Deschamps JD, van der Donk WA, Holman TR (2009b) Kinetic and structural investigations of the allosteric site in human epithelial 15-lipoxygenase-2. *Biochemistry* 48:8721–8730
- Wuest SJ, Horn T, Marti-Jaun J, Kühn H, Hersberger M (2014) Association of polymorphisms in the ALOX15B gene with coronary artery disease. *Clin Biochem* 47:349–355
- Yoshiyuki K, Hiromichi O, Shigeru A, Kimiye B, Mitsugi K (1985) Inhibition of the formation of 5-hydroxy-6, 8, 11, 14-eicosatetraenoic acid from arachidonic acid in polymorphonuclear leukocytes by various coumarins. *BBA-Lipid Lipid Met* 834:224–229